Closed-Loop Class E Transcutaneous Power and Data Link for MicroImplants

Philip R. Troyk, *Senior Member, IEEE*, and Martin A. K. Schwan

Abstract—**Magnetic transcutaneous coupling is frequently used for power and data transfer to implanted electronic devices. The proposed development of MicroImplants, small enough to be injected through a hypodermic needle suggest the need for a high-efficiency magnetic transcutaneous link. This paper describes the use of a multifrequency transmitter coil driver based upon the Class E topology. The development of a "high-Q approximation" which simplifies the design procedure is presented. A closed-loop controller to compensate for transmitter and receiver variations, and a method of data modulation, using synchronous frequency shifting are described. The closed-loop Class E circuit shows great promise, especially for circuits with unusually low coefficients of coupling. Currents of several amperes, at radio frequencies, can easily and efficiently be obtained.**

Introduction

RECENTLY, there has been interest in a new type of neural prosthetic device known as a "Microimplant" [1]. Based upon designs of transponders from the electronic identification industry, the microimplant would be small enough to be injected through a 14 gauge (1.6 mm) hypodermic needle. Uses would include neural-muscular stimulation, and telemetry for multichannel neural electrodes or other biological sensors. For neural-muscular stimulation, the microstimulator would consist of a one-channel, addressable, bipolar stimulator. It would be powered by transcutaneous magnetic coupling, using one large external transmitter coil to power and communicate with as many as 100 implanted microstimulators per limb. The receiver coil contained within the microstimulator would be millimeter- or submillimeter-sized. The coupling conditions for this type of device are extremely unfavorable, with the coupling coefficient in the range of $10^{-5} < k < 10^{-3}$. Due to this extremely low k, the loading effects on the external transmitter from the reflected impedance of hundreds microstimulators can be minimal [1].

For Microimplant telemetry, it has been suggested that printed, thin-film coils, integrated directly with the sensor circuitry would provide significant manufacturing and performance advantages. For such devices, the coupling coefficient could be up to two orders of magnitude smaller than that for the microstimulator. In addition, it would be unlikely that the integrated coil would have a high Q.

One method of compensating for the extremely unfavorable power transfer conditions is by the generation of a high-intensity magnetic field at radio frequencies. For reasons of portability, it is often important to design transcutaneous coil transmitters using light-weight battery power. This paper focuses on the use of multifrequency networks, in a Class E switch-mode converter topology to obtain unusually high transmitter coil currents at frequencies ranging from hundreds of kilohertz to several megahertz.

Design Factors for Transcutaneous Links

There are many factors to consider when designing a transcutaneous link for an implant: size and shape of the coils, location of the implant, misalignment and displacement tolerance, power and regulation requirements, efficiency, communication bandwidth, complexity of receiver circuitry, and complexity and bulk of transmitter circuitry and power supply. Each application has its own unique requirements which determine the priority of these factors. Often, the implanted device is designed first, and then the transcutaneous link is designed to accommodate it. Efficiency, displacement tolerance, and communication are usually the main focus of the design. Maximizing the first of these reduces the bulk of the transmitter power supply. Maximizing the second reduces the required receiver regulation.

There have been several analyses and approaches to the design of magnetic transcutaneous links [1]–[4]. These design approaches attempt to maximize coupling efficiency and displacement tolerance through the design of the transmitting and receiving coil circuits.

Donaldson *et al.* [2] explain that efficiency and displacement tolerance are opposing design tradeoffs. For given coil Q's and coupling coefficient, k, maximum coupling efficiency occurs at a point where the displacement tolerance is quite poor. Galbraith *et al.* [3] describe a common design approach called the geometric approach. Here both the transmitter and receiver coils are circular and planar, with the receiver coil smaller than the transmitter coil. As long as the receiver coil is within the perimeter of the transmitter coil, the coupling coefficient will remain fairly constant. In this approach the coils can be

Manuscript received May 28, 1990; revised December 12, 1992.

The authors are with the Pritzker Institute of Medical Engineering, Illinois Institute of Technology, Chicago, IL 60616.

IEEE Log Number 9108125.

moved, within parallel planes and with minor rotations, without a significant change in k. Since the magnitude of the receiver voltage is dependent on the coupling coefficient, k, this approach allows for lateral displacement tolerance. Galbraith *et al.* also explain that for the near field, the coupling coefficient drops-off proportional to the separation of the coils. Therefore the geometric approach is not separation-tolerant. The performance cost of this semi-tolerant design is that the absolute coupling is reduced. In order to obtain a desired receiver voltage, the transmitter coil must carry a larger current than it would if the coils were more equally sized. Larger transmitter currents have historically resulted in higher I^2R losses, due to transmitter inefficiencies, and increased the bulk of the external circuitry and batteries.

Donaldson *et al.* describe the "critical coupling," k(crit), method for transcutaneous coils in which the reflection of the secondary impedance, in the primary circuit, is real for all values of coupling coefficient, k. This approach minimizes the change in reactance of the primary transmitter coil for changes in the secondary (receiver) load conditions, and tends to compromise between maximizing voltage transfer, and minimizing coil displacement effects.

Galbraith, *et al.* also describe a method of desensitizing the voltage transfer ratio, or to use their terminology, link gain. Their method involves stagger tuning. This method provides displacement tolerance, efficiency, and wide bandwidth. The main feature of this method is that both the transmitter and receiver circuits are tuned off the operating frequency, one above and one below. Galbraith *et al.* note that the poles shift when the coupling coefficient varies. If the poles are properly placed, they shift in a manner that compensates the link gain for the change in coupling. In effect, proper tuning results in a variation of the reflected impedance for changes in coupling coefficient. The effect of increased coupling would be to increase the link gain. The effect of increased reflected impedance would be to lower the generated magnetic field. These two effects cancel each other and produce a link gain that is fairly insensitive to the coupling coefficient and therefore displacement tolerant.

Unfortunately, both these approaches provide little benefit for systems with unusually low values of k. Donaldson *et al.* have shown that both coupling efficiency and voltage transfer ratio are extremely low if k(crit) is more than one order of magnitude larger than k. A high k(crit)$/k$ ratio typically compromises the efficiency of the active output driver stage. As pointed out by both Donaldson *et al.* [2] and Heetderks [1], maximum voltage transfer between two coils occurs when the receiver coil is tuned to the transmitter frequency.

Fundamentals of Driving Transcutaneous Coils

The magnitude of the magnetic field resulting from ac current in a coil is dependent upon coil geometry and on the ampere-turns product of the coil. Increasing the turns on a coil increases its inductance, with inductance being proportional to the square of the turns.

The magnitude of voltage across a coil with an ac current, I, driven through it is given by the familiar expression:

$$|V| = |I| * \sqrt{(R_{esr}^2 + (\omega L_1)^2)} \quad (1)$$

where R_{esr} is the equivalent-series-resistance of the coil, ω is the driving radian frequency, and L is the inductance of the coil. V will be large at high frequencies due to the large reactive component. Typically coils are not driven directly because the active driver must handle both the requisite high current and high voltage, which is very inefficient. Fig. 1 shows three networks used with transmitter coils to produce more favorable load conditions for the active device of the driver.

The first load network of Fig. 1(a) places a capacitor in series with the coil and the pair is driven at their resonant frequency. This is the most commonly used configuration: series resonance. At resonance the reactances of the coil and capacitor cancel each other and the impedance of the network is reduced to the sum of the equivalent-series-resistances (ESR) of the windings of the coil and the capacitor. This impedance cancellation reduces the voltage that the driver must handle; however, the active device must still handle the large coil current. For low-loss coils and capacitors, the voltage drop across the series ESR of the coil and capacitor can be significantly less than the saturation drop of the active driver. Therefore, for large primary coil currents, the power in the driver becomes dominant and excessive.

For the series resonant circuit, the magnetic field, produced for a fixed coil current, can be increased by increasing the coil inductance. To increase L_1, more turns could be added to the transmitter coil. Adding more turns will increase R_{esr} due to both the additional wire length and proximity-effect current crowding. One strategy to maintain or reduce R_{esr} might be to increase wire size or use Litz wire. However, increasing L_1 (without increasing R_{esr}) would require that the Q of the primary circuit be impracticably (if not impossibly) high.

Increasing coil current by simply lowering R_{esr} would require drastic reductions in the output resistance of the driver circuit and the winding resistance of the coil. For typical driver circuits, such a reduction is not practical. Furthermore, low-resistance active devices, tending to have large die areas, would be characterized by large input capacitances which would raise the power handling requirements of the predriver stage.

The second load network, shown in Fig. 1(b), lowers the current the active device must handle by means of parallel resonance. In this configuration, a capacitor is placed in parallel with the transmitter coil, and the pair is again driven at their resonant frequency. At resonance, the reactances cancel and the impedance is simply the series-to-parallel transformed resistances of the coil and capacitor in parallel. The transformed resistance (R_p) is de-

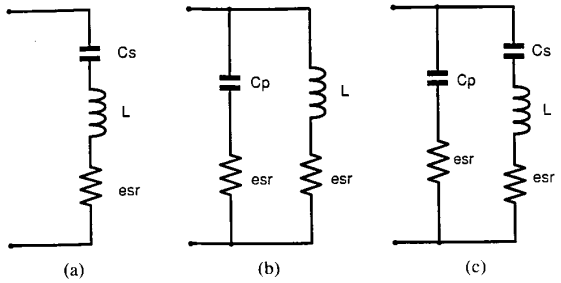

Fig. 1. (a) Series-resonant model for a transmitter coil. (b) Parallel-resonant model for a transmitter coil. (c) Multifrequency load network for transmitter coil L.

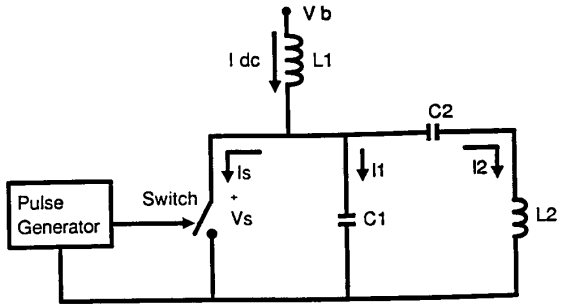

Fig. 2. Class E driver circuit topology. The use of the multifrequency load network provides a unique driving impedance shown in Fig. 3.

scribed by:

$$R_p = R_s(1 + Q^2) \tag{2}$$

where Q is the quality factor of the circuit, and R_s is the original series resistance. If Q is large, R_p is also large, therefore reducing the amount of current the active device must handle. The large ac current, required in the coil for the large magnetic field, results from the resonance of the coil and the capacitor. The parallel resonant load network, however, has the disadvantage of requiring the driver to handle large voltages, and high-voltage active devices have correspondingly high capacitances, limiting the operating frequency.

The advantages of both of the previous two networks are present in the third, shown in Fig. 1(c). This load network is a combination series-parallel resonant circuit, and commonly referred to as a "multifrequency network." For this type of load network, the active device handles both low current and low voltage, producing very favorable load conditions for the active device, and a means of producing large coil currents.

Class E Coil Driver

The Class E driver [5], shown in Fig. 2, uses a multifrequency load network, takes advantage of the impedance transformation inherent to this network, and is a switched-mode resonant driver; the active device acts as a switch. The driving point impedance seen by the active device has the frequency response shown in Fig. 3. The valley in the frequency response is caused by the series resonance of L_2 and C_2. As the frequency increases, the reactance of L_2 and C_2, in series, is positive which, with C_1, forms the parallel resonant peak.

When the circuit is operated between the series and parallel peaks, there is a particular frequency where the power losses in the driver are minimized. This operating point, called the Class E point or Class E mode, is characterized by voltage and current waveforms which are 180° out of phase. A finite value of one is accompanied by a near-zero value for the other. This results in nearly zero power loss in the switch. The circuit operation under these conditions can be described as follows: The current in the L_2-C_2 branch is nearly sinusoidal with a frequency equal to that of the switch drive. This is a consequence of the high Q of the branch. While the switch is closed, L_2 and C_2 supply current back to the switch (i.e., I2 is negative), no current flows through C_1, and the voltage across the switch is zero. When the switch opens, L_2 and C_2 continue supplying current (i.e., I2 is still negative), however this current now flows through C_1 resulting in a positive voltage across the switch. When the current in the L_2-C_2 branch reverses (i.e., I2 becomes positive), the charge on C_1 supplies the current, reducing the voltage across the switch. When the voltage across the switch becomes zero the switch is closed and the cycle is repeated. The inductor L_1, in series with the power supply, acts as a constant current source, supplying the energy dissipated during each cycle. At a specific operating frequency, (i.e., Class E point) the switch voltage and L_2 current are close to 90° out of phase and the voltage across the switch (i.e., active device), Vs, has a value of zero with zero slope, just as the switch closes. This ensures there will be no large peak currents in the switch and minimizes the switching losses of the driver. Fig. 4 shows PSPICE drive, voltage, and switch-current waveforms for a Class E driver operating in the minimized loss mode near 1 MHz. Analyses of the Class E circuit have been done by: Sokal *et al.*, Gutmann *et al.*, and others [5]–[11].

The optimum operating mode of the Class E driver, as noted above, is characterized by minimized loss. This occurs when the switch voltage has a value of zero with zero slope just before switch closure on every cycle. The zero voltage level prevents large current surges in the switch, minimizing switching losses. The zero slope allows for slight timing errors or slow switch closure. If the voltage across the switch is not zero at switch closure there will be power losses due to the simultaneous large current through and voltage across the active device.

Switched-mode resonant circuits often have the disadvantage of a limited frequency range due to the switch capacitance. The Class E driver is immune to this problem because the switch capacitance can be compensated for by modifying the value of the parallel capacitor (C_1). Since there is no voltage on the switch at switch closure, no charge resides on the switch "capacitor" and minimal switching time is required to close the switch, with no

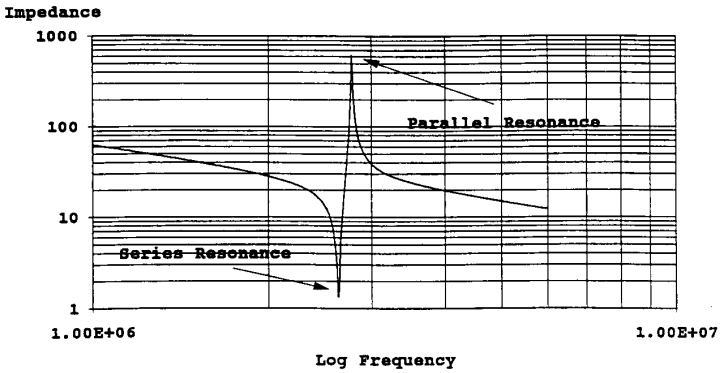

Fig. 3. Driving impedance of a typical multifrequency load network. The Class E frequency is located between the series and parallel peaks.

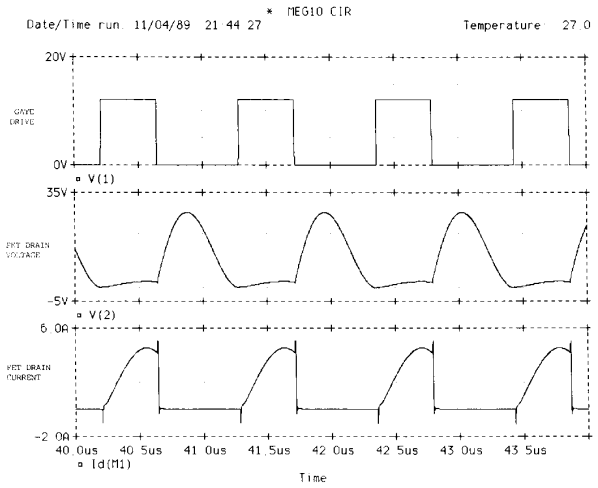

Fig. 4. PSPICE gate drive, Fet drain (switch) voltage, and Fet drain (switch) current for a Class E converter.

switching losses. The simple one-transistor topology eliminates the primary cause of frequency limiting in most switch-mode circuits—switch dead time to avoid cross conduction. In the common push-pull topology, dead time (a short time during which both transistors must be off) is necessary to prevent the transistors from conducting simultaneously (cross conduction), and consequently dissipating a large amount of instantaneous power.

A priori determination of the exact Class E point is difficult. Redl *et al.* [7] has given design information for 50% duty cycle. However, for high-Q loads, characteristic of low-loss transcutaneous coils, smaller duty-cycles (10–20%) are more appropriate. A "high-Q approximation" design procedure can be used, and is reasonably valid near the Class E point.

High-Q Approximation

For a given combination of component values, the Class E frequency is dependent on the quality factor of the load network, i.e., minimum-loss operation occurs for a critical network Q.

Referring to Fig. 5, when the switch is opened, the switch voltage follows the form of a damped sinusoid which would settle out to the supply voltage V_B if the switch did not close again. During Class E operation, the switch closes at the first negative peak in the "ringing." At the negative peak of the switch voltage, the voltage value and slope are zero, thus minimizing switching losses. When the network Q is too high, the "ringing" of the switch voltage does not damp sufficiently and would cause the switch voltage to have a negative peak below zero. Under these conditions, the unidirectional nature of the semiconductor switch results in conduction, usually due to a protection diode. If the Q is too low the "ringing" of the switch voltage is excessively damped and the switch voltage does not return to zero resulting in a negative peak above zero. Since the Q of the circuit is dependent on the frequency, and a critical Q is required for minimum-loss operation, there is but one frequency for a given network which can maintain the Class E conditions. This frequency is between the series and parallel resonant network peaks, and is analogous to staying within region 4 described by Redl *et al.* in [7]. Kazimierczuk *et al.* [11] and others have made reference to a critical (or minimum) Q required for Class E operation; however, no closed form solutions have appeared in the literature.

The use of a high-Q (>80) coil, low ESR capacitors, and a low on-resistance switch means that the switch waveform will be characterized by very little damping. Under these conditions, the switch waveform V_s can be approximated as a raised cosine wave:

$$V_s = (A/2) - ((A/2)\cos(\omega_p t)) \quad \text{for } t' \le t < t' + T_p$$
$$0 \quad \text{for } t' + T_p \le t < t' + T_o \qquad (3)$$

where A is the peak amplitude of the switch voltage, ω_p is the parallel resonance frequency, $T_p = 2\pi/\omega_p$, $T_o = 2\pi/\omega_E$, and ω_E is the Class E frequency.

Using Fourier analysis, the fundamental V_s', and the dc component V_b, of the switch waveform (3) can be expressed as functions of the peak switch voltage A, and the

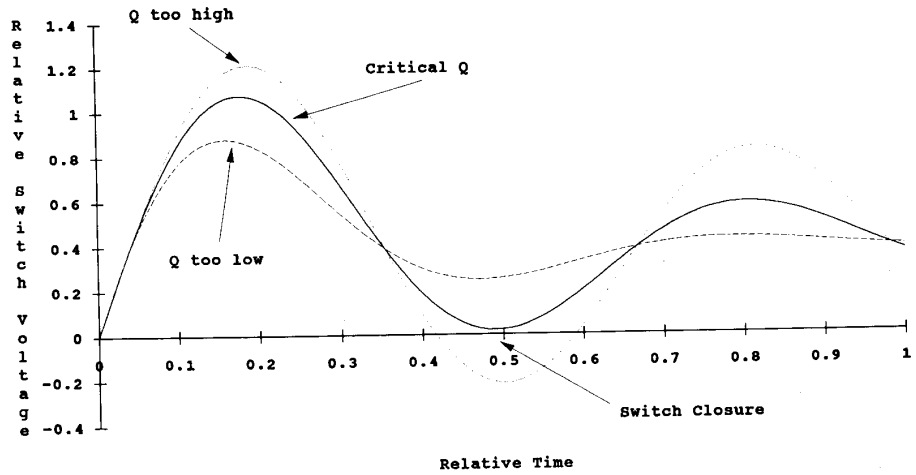

Fig. 5. Switch voltage for three different circuit Q's. The optimal (critical Q) provides zero voltage, with zero slope at the time of switch closure.

switch Duty Cycle, D:

$$V_b = (A/2)(1 - D) \tag{4a}$$

$$V_s' = (A/2\pi)(1/(2D - D^2))\sqrt{(\sin^2(2\pi D) + \cos(2\pi D) - 1)^2}). \tag{4b}$$

The design procedure can then be described as follows: Given:

Transmitter coil inductance, L_2, and Q_1,
Desired peak coil current, I_2,
The frequency of operation, ω_E,
The switch duty cycle, D,
The power supply voltage, V_b.

The peak switch voltage A can be computed from (4a), and the fundamental component of the switch voltage, V_s' can be computed from (4b). (Note that in the range of $D < 0.25$, V_s' is approximately 0.5 * A) The coil resistance is found from

$$R_c = \omega_E L_2 / Q_1. \tag{5}$$

The series branch impedance is found from

$$|Z_s| = V_s'/I_2. \tag{6}$$

The reactance of the series branch is found from

$$X_s = \sqrt{(Z_s^2 - R_c^2)}. \tag{7}$$

The value of C_2 is found from

$$C_2 = 1/(\omega_E(\omega_E L_2 - X_s)). \tag{8}$$

The value of C_1 is found from

$$C_1 = 1/(\omega_E X_s). \tag{9}$$

The dc choke, L_1, is chosen to be three to ten times greater than L_2.

Closed-Loop Control of the Class E Converter

In transcutaneous inductive link systems, where the coupling coefficient is appreciable, changes in the device load would affect the Q of Class E driver. Due to the high sensitivity of Class E circuits to changes in load Q, the driver can move out of the Class E lossless mode of operation, if some means of frequency adjustment based on load variations is not included. For Microimplants, large changes in the individual receivers would have only a minute effect on the transmitter Q. However, other external influences on the transmitter coil could significantly shift its inductance and resistance. There are two primary mechanisms responsible for shifts in the transmitter coil characteristics: 1) Proximity of the transmitter coil, to metallic objects. 2) Mechanical deformation of the transmitter coil. In the first case, inductance as well as resistance changes can occur, depending upon the shape and composition of the metal object. In the second case, small changes in the shape of the coil can produce large inductance variations. Both of these effects can seriously shift the operating point of the Class E converter. Failure to provide some means of frequency/duty cycle adjustment to accommodate the new operating point can result in dramatic increases in the power dissipation of the active switch, with probable device destruction.

Table I presents the nominal coil inductance and resistance, for a 12 turn, 9 cm diameter coil, as well as variations in their values for coil deformations and adjacent metal pieces such as those which might be used in a wheelchair. These measurements were made using a Solartron 1260 Impedance/Gain-Phase Analyzer.

Case 1 is the transmitter coil suspended away from external metal objects, without any mechanical deformation. Case 2 is the transmitter coil placed perpendicular to a 5 in. square copper plate. Case 3 is the transmitter coil laid face down on a copper plate. Case 4 is the transmitter coil coupled to a 9 cm coil driving a resistive load,

TABLE I

Coil Conditions	Circuit Parameter	
	Inductance (uH)	Equivalent Series Resistance (Ω)
1) Coil in Air	30.29	1.02
2) Coil w/perpendicular Cu Plate	28.42	1.20
3) Coil w/parallel Cu Plate	16.03	2.07
4) Coil w/Coupled Load	29.73	15.50
5) Elliptical Coil (8 × 11) cm	29.86	1.09
6) Saddle Coil	29.40	1.08

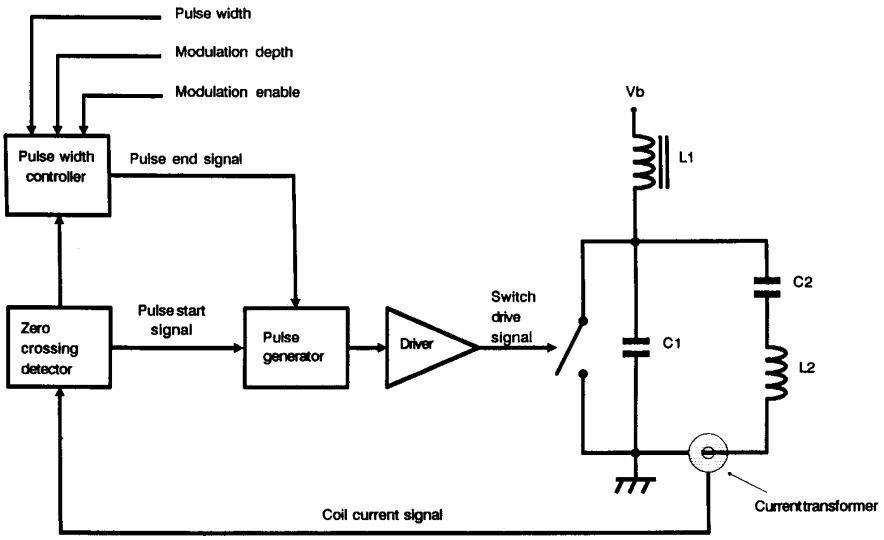

Fig. 6. Block diagram of Class E converter with coil current zero-crossing controller. See text for explanation of system operation.

and is included to show the effects of reflected resistive changes without significant inductance changes. Case 5 is the transmitter coil deformed into an ellipse of dimensions 8 × 11 cm. Case 6 is the transmitter coil bent into the shape of a saddle. Case 3 is an extreme condition and illustrates dramatic shifts in inductance as well as resistance. A more typical condition would be case 2 combined with 5 and 6 which is representative of changes resulting from deformations of a coil contained in a garment, being moved next to the arm of a wheelchair, wristwatch, metal table, or other furniture.

In analyzing the optimal time point of switch closure, for the Class E converter, the lowest switching power loss occurs when the switch is closed at the first negative peak of the switch voltage. This suggests using the zero-crossing of the switch-voltage derivative to control switch closure. Using an active circuit to obtain the derivative might be one approach. A second method is to recognize that for a sinusoid, the integral and derivative differ only by their sign. Due to the high Q of the series branch C_2-L_2, the current through L_2 is approximately equal to the switch-voltage negative derivative. This current can be easily sensed using a current-sense toroid, and its zero-crossing used to time the leading edge of the switch drive waveform.

This approach is shown in Fig. 6. By using the negative zero-crossing of the coil current to trigger the switch drive, the switch always closes at precisely the correct instant to maintain minimal switching losses. The Class E point, for which near-zero loss occurs, is obtained at one particular combination of frequency and duty cycle. The Class E frequency is identical with the frequency maintained by the coil current zero-crossing controller and results in zero-slope at switch closure. The Class E duty cycle produces zero absolute voltage at switch closure. The Pulse generator also serves as a "start-up" circuit. Immediately following power-up, the pulse generator excites the multifrequency network at a frequency lower than the Class E frequency. This produces sufficient current in L_2 to create a feedback signal for the controller.

Changes in the coil inductance require corresponding shifts in the converter operating frequency, in order to maintain Class E operation. The coil current zero-crossing controller compensates for coil inductance changes.

TABLE II

	Supply I (mA)	Peak Switch P (W)	Avg. Switch P (W)	Peak Coil I (A)	Coil I/P.S. P (AT/W)
OPEN LOOP					
1	40.6	0.068	0.0035	0.726	23.8
2	422.5	265.2	2.636	1.227	3.87
3	272.4	258.6	2.447	0.116	0.567
4	170.2	129.2	0.796	0.304	2.38
5, 6	155.2	37.62	0.195	1.334	11.4
2, 5, 6	251.4	93.21	0.539	1.355	7.18
CLOSED LOOP					
1	38.0	0.140	0.0024	0.718	25.1
2	43.7	0.023	0.0038	0.745	22.7
3	134.7	15.220	0.047	1.000	9.89
4	170.3	290.3	0.791	0.299	2.34
5, 6	39.6	0.161	0.0028	0.734	24.7
2, 5, 6	50.9	1.976	0.0017	0.703	18.4

As the natural frequency of the network rises (due to reductions in coil inductance), the time from switch opening to the load current zero-crossing decreases, however, the controller maintains the phase relationship between switch-closure and load-current zero-crossing. Therefore, the controller appropriately shifts the operating frequency to the new Class E frequency by controlling the interpulse interval of the switch drive.

Changes in coil resistance due to reflected variations in implant load conditions would be minimal for Microimplants [1]. Increases in coil resistance due to proximity of metal objects would typically be accompanied by decreases in coil inductance. The upwards shift in converter frequency would also result in a duty cycle increase since the switch on-time is fixed. In this regard, the coil current zero-crossing controller behaves as a mixed frequency/duty cycle controller.

Table II shows the predicted changes in average supply current, peak switch power, average switch power, and peak fundamental coil current, as determined from PSPICE simulations, for a typical Class E converter operating at 760 kHz. The transmitter coil model used was a series *L-R* circuit with values as listed in Table I. Listed are values for open-loop fixed frequency/duty cycle, and closed-loop partially compensated duty cycle operation, for each, and combinations, of the cases listed in Table I.

In examining the data in Tables I and II it can be seen that seemingly small changes in the coil inductance and resistance can have dramatic effects upon circuit operation, particularly the power dissipated by the switch. The use of the coil-current zero-crossing controller provides a significant reduction in the average and peak switch power. Efficiency was determined by dividing the peak coil current-coil turns product by the power supplied from the battery source, and is listed under COIL I/P.S. P (AT/W) in Table II.

Data Modulation

Most transcutaneous links require some form of modulation for communication with the implant. For the high-Q Class E driver, coil current amplitude modulation is feasible through synchronous frequency modulation. The high variation in the C_2-L_2 series-branch impedance with changes in frequency can be exploited to modulate the coil current. Due to the steepness of the impedance curve, variations on the order of 0.1% in frequency can produce changes of up to 10% in coil current. This amplitude modulation of the coil current is an attractive method of data transmission. It will not interfere with the transfer of power to the implant because the coil current and therefore magnetic field, and coupled power, never fall below the nominal value. Although the Class E driver is periodically moved off the optimum operating point the increase in power dissipation is insignificant. Using this method a practical modulation range of 5–10% can be achieved.

A disadvantage of data transfer by modulation of current amplitude in any high-Q driver is limited bandwidth or bit rate. Because of the high Q of the driver, an abrupt change in frequency will require several cycles for the coil current to reach its new steady state value. The use of *synchronous* frequency modulation, where the change is synchronized to the operating frequency, limits the transient to the time required for the current in L_1 to adjust to the new value. This response time can be reduced by lowering the value of the dc choke, L_1.

For the closed-loop, zero-crossing controlled Class E converter, synchronous frequency modulation can be easily accomplished by changing the on-time of the switch drive, or offsetting the current-sense toroid output. Controlling the former has some advantages. Since the off-time of the switch is controlled by the network natural frequency, via the current feedback, changing the on-time shifts the total cycle time, and therefore the operating frequency. The appropriate inputs are illustrated in Fig. 6.

Experimental Methods

Using the design procedure outlined above, a Class E driver was designed with the following specifications:

Transmitter Coil: 12 turns of #200/38 Litz wire, 9 cm diameter, Coil Inductance = 30 μH, Q = 110.
Coil current: 0.7 Apk
Frequency: 760 kHz
Switch Duty Cycle: 0.12
Power Supply: 9.0 VDC

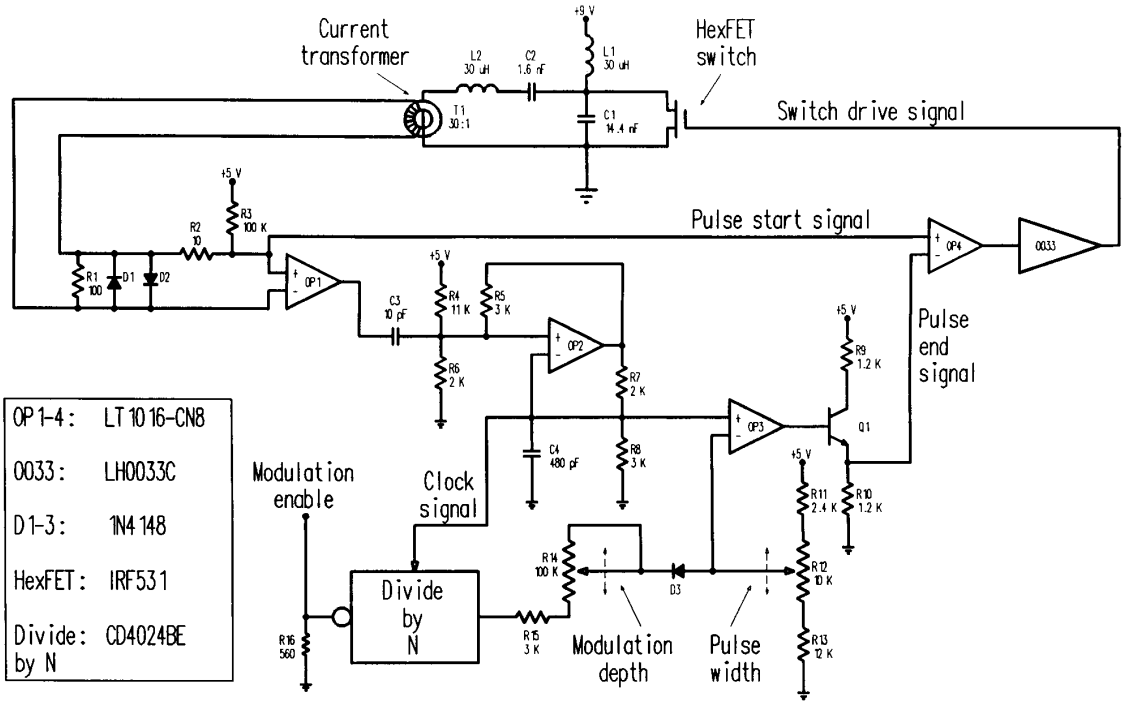

Fig. 7. Schematic diagram of coil current zero-crossing controlled Class E laboratory model. The current transformer T1 provides the feedback signal used to keep the converter operating near the Class E point.

The following parameters were calculated:

$$C_1 = 14.4 \text{ nF}$$

$$C_2 = 1.6 \text{ nF}$$

$$L_1 = 50\ \mu\text{H}$$

A schematic of the completed circuit is shown in Fig. 7. OP1-OP4 are LT1016-CN8 Ultra Fast Precision Comparators, 0033 is a LH0033C Fast Buffer Amplifier, and the HexFet is an IRF531. The Divide-by-N circuit is a CD4024BE 7 stage binary counter with Dip switches to set N to 8, 16, or 32. Polystyrene capacitors were used for C_1 and C_2. The 5 V supply was derived from the 9 V supply using a Zener diode clamp. The 5 V supply was necessary for the "fast" active devices, OP1-OP4. Care was taken to minimize lead length, using standard radio-frequency type construction techniques. In particular, the lead length from the FET drain to C_1 was made as short as possible. Any finite lead length for this connection results in ringing at switch shutoff due to the lead inductance. The capacitors demonstrated a frequency dependence, due to their self-resonance, and appropriate value corrections were made. Multiple capacitors, in parallel, were used for both C_1 and C_2, raising the effective component resonant frequency to well above the operating frequency. FET gate drive was provided by an LH0033 buffer, driven by a coil current zero-crossing controller. Operation of the circuit is as follows.

R7, R8, C3, C4, and OP2 comprise a relaxation oscillator, the frequency of which is set lower than the design Class E frequency of 760 kHz. At power-up, the current through L_2 is zero, and there is no current feedback signal at the output of T_1. R2 and R3 bias the noninverting inputs of OP1 and OP2 with ≈ 4 mV in order to avoid chatter. The relaxation oscillator produces an exponentially varying waveform at the input of OP3.

In the absence of a modulation enable, R12 sets the switch point for comparator OP3. Thus when the voltage on C_4 falls below the voltage at R12, the inverting input to OP4 is below the noninverting input and the HexFet gate drive is high, turning on the switch. When the voltage on C_4 rises above that of R12, the switch turns off. In this open-loop mode, the relaxation oscillator controls both the frequency and on-time of the switch drive.

As the magnitude of the ac current flowing in the C2-L2 branch increases, the current transformer T_1 produces a square voltage signal across R1, due to the clipping action of D1 and D2, which is 180° out of phase with the current in the C2-L2 branch of the converter. As this current crosses zero and the square wave goes positive both OP1 and OP4 switch to the high state, closing the converter switch. Since the natural frequency of the relaxation oscillator is lower than the Class E frequency, the leading edge of the output of OP1 serves to synchronize the relaxation oscillator. OP3 switches high, after a delay determined by OP2, and the voltage at the inverting input of OP4 is pulled high by Q1 resulting in the termination of the switch drive pulse, opening the converter switch. Thus, OP2 serves initially to start the converter, then functions as a pulse duration circuit. It is essential to min-

TABLE III

	Circuit Parameter				
	Peak Coil I (A)	Peak Switch Voltage	Frequency	Power Supply I (A)	Duty Cycle
Calculated	0.7	20.45	760 K	0.0328	0.12
PSPICE Model	0.718	19.27	758.5 K	0.038	0.12
Measured	0.72	19.2	760 K	0.038	0.125

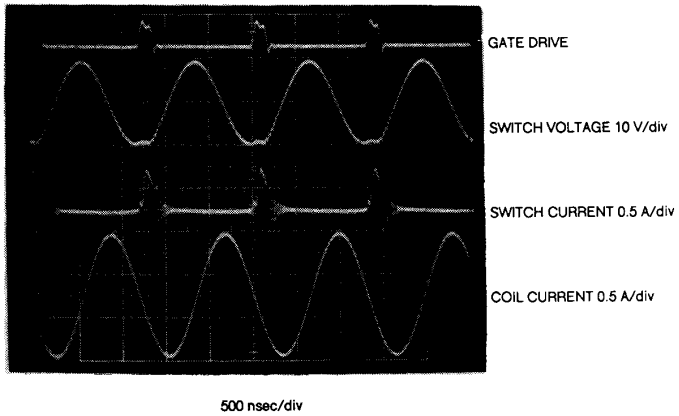

Fig. 8. Oscilloscope photograph of laboratory Class E coil driver waveforms, for a 9 cm coil. The operating frequency is 760 kHz, and the coil current-turns product is 8.4 AT.

imize the delay between the current zero-crossing and the leading edge of the switch drive. This is accomplished by the direct path from T_1 to OP4, with the indirect path, via OP1, OP2, OP3, and Q1, acting to determine the pulse duration.

When D3 is reverse biased, the Divide by N circuit output is high, the voltage at the inverting input of OP3 is determined solely by the setting of R12. During modulation, when the output of the Divide by N circuit is low, R14 and R15 shunt the lower half of the R11-R12-R13 voltage divider, lowering the reference voltage at the inverting input of OP3 and consequently decreasing the switch-drive pulse duration.

Measurements of coil current and switch voltage were done using a Tektronix P6022 current probe, and a Tektronix 7623A oscilloscope. The value of L_1 was made unusually low, to minimize the transient response time during modulation. The lower the value of L_1, the higher the ac component of the power supply current, and consequently the high-frequency losses of the choke are increased. For the choke used the R_{esr} was approximately 1 Ω, resulting in negligible power losses.

Results

The circuit performed as per the design specifications. Comparisons between calculated, PSPICE simulated, and measured values of frequency, voltage, and current are found in Table III.

For the PSPICE and the Measured values, the simulation and the laboratory breadboard were operated using the closed-loop coil current zero-crossing controller. Therefore, the data for these cases were obtained from the stable operating point provided by the controller.

All values were in excellent agreement, demonstrating the utility of the high-Q approximation. Oscilloscope photographs of the coil current, switch voltage, and switch current are shown in Fig. 8. Note the lack of simultaneous switch voltage and current, and the zero-slope of the switch voltage at switch turn-on. The coil current was very close to the design value of 0.7 Apk, and could easily be modified by changing the value of C_1 or by slight shifts in the operating frequency.

Modulation of the current is shown in Fig. 9. This was accomplished using $N = 32$ in the divide-by-N modulation circuit. The upper trace shows the modulated coil current, and the lower trace shows the modulation signal. A modulation depth of 20% of peak was obtained for a frequency shift of 0.5%. The transient settling time was approximately 8 μs, or 6 cycles of the carrier.

The effects of changing coil characteristics were determined by replicating the conditions presented in Table I. Only the closed-loop circuit was used since the increases in switch power dissipation for the open-loop circuit quickly lead to FET destruction. Comparisons between the PSPICE predicted, and measured, power supply current, peak coil current and operating frequency for differing cases of coil parameters, from Table I, are presented in Table IV.

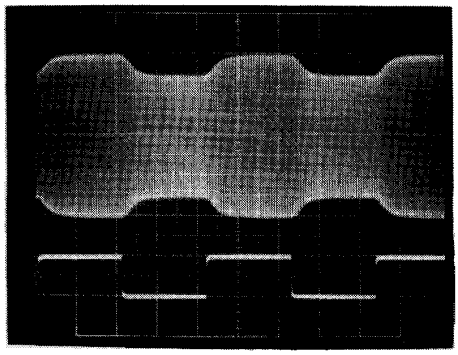

Fig. 9. Oscilloscope photograph of modulated coil current for the converter of Fig. 6. The modulation depth is 20% of the peak for a frequency shift of 0.5%. Settling time is approximately six carrier cycles.

TABLE IV

	Supply I (mA)	Peak Coil I (A)	Frequency (kHz)
MEASURED			
1	38.0	0.726	760
2	42.0	0.710	776
3	130.0	0.84	1000
5,6	38.0	0.72	762
2,5,6	42.0	0.71	779
PSPICE			
1	38.0	0.718	759
2	43.7	0.745	783
3	134.7	1.000	1039
5,6	39.6	0.734	769
2,5,6	50.9	0.703	772

Discussion

The use of $V_s' = A/2$ seems to be an adequate approximation for computing the value of the switch waveform fundamental component. This was used for several test cases, which were subsequently checked using PSPICE simulations, with very close agreement between the calculated and the simulated circuit responses. The use of the high-Q approximation provides a significant simplification of the Class E design process, minimizing the need for iterative design. The fundamental basis for the assumption lies with the approximation of the switch waveform as a raised-cosine wave followed by a period of zero magnitude (during switch closure). The use of the raised-cosine simplifies the Fourier analysis. For lower series-branch Q's (<40), the switch waveform is better described by a damped sinusoid.

The performance of the circuit was impressive, considering the relatively high-magnitude of coil current. The coil current zero-crossing prevented excessive FET power dissipation by appropriately changing the leading edge of the gate drive. For this technique, it is essential to minimize the propagation delay from the positive zero-crossing of the coil current to the leading edge of the gate drive. Several circuit parameters affect this delay.

The phase shift of the current-sense toroid must be minimized. This is accomplished by using a relatively low-valued burden resistor. Diode clamping of the toroid output may also be helpful.

The propagation delay of the comparator and gate driver must be minimized. This requires the use of high-speed components. In the design shown in Fig. 7, a minimal active component path is provided from T_1 to the FET gate. The high-current LH0033 driver was required to charge the FET gate capacitance.

The IRF531 FET was chosen for its current handling capability, and its low gate capacitance. Note that the drain-to-source capacitance is shunted by C_1, and therefore is not a limiting factor in the upper frequency limit of the converter.

The closed-loop converter is virtually essential for accommodating changes in the inductance and resistance of the transmitter coil. As demonstrated in Table II, the open-loop converter is characterized by unacceptably high values of power dissipation for minor changes in transmitter coil conditions. The coil-current zero-crossing controller allows for use of the Class E topology in realistic applications outside a controlled laboratory environment. We have also found that using the controller for PSPICE simulations significantly reduces the number of iterations to obtain a usable simulation.

Differences between the measured and PSPICE predicted shifts in converter operation as presented in Table IV, are most likely due to shifts in the effective capacitance values of C_1 and C_2. The capacitance shifts with increasing frequency result from the self resonances of the capacitors.

Conclusions

The Class E driver is a highly efficient network for producing large radio-frequency currents in transcutaneous magnetic coils. The simplicity of the topology makes it attractive not only for systems with extremely low coefficients of coupling, but also for portable devices needing

high efficiency. The Class E circuit is ideally suited for high-Q loads, and the use of the High-Q approximation simplifies the design procedure. The use of coil current zero-crossing control provides excellent stability of the operating frequency even for changes in the coil inductance and resistance.

REFERENCES

[1] W. J. Heetderks, "RF powering of millimeter- and submillimeter-sized neural prosthetic implants," *IEEE Trans. Biomed. Eng.*, vol. BME-35, pp. 323-327, May 1988.

[2] N. de N. Donaldson and T. A. Perkins, "Analysis of resonant coupled coils in the design of radio frequency transcutaneous links," *Med. Biol. Eng. Comput.*, no. 21, pp. 612-627, Sept. 1983.

[3] D. C. Galbraith, M. Soma, and R. L. White, "A wide-band efficient inductive transdermal power and data link with coupling insensitive gain," *IEEE Trans. Biomed. Eng.*, vol. BME-34, pp. 265-275, Apr. 1987.

[4] M. Soma, D. C. Galbraith, and R. L. White, "Radio-frequency coils in implantable devices: misalignment analysis and design procedure," *IEEE Trans. Biomed. Eng.*, vol. BME-34, pp. 276-282, Apr. 1987.

[5] N. O. Sokal and A. D. Sokal, "Class E—a new class of high efficiency tuned single-ended switching power amplifiers," *IEEE J. Solid-State Circ.*, vol. 10, pp. 168-176, June 1975.

[6] M. K. Kazimierczuk and K. Puczko, "Exact analysis of Class E tuned power amplifier at any Q and switch duty cycle," *IEEE Trans. Circ. Syst.*, vol. 34, pp. 149-159, Feb. 1987.

[7] R. Redl, B. Molnar, and N. O. Sokal, "Small-signal dynamic analysis of regulated Class E dc/dc converters," *IEEE Trans. Power Elec.*, vol. PE-1, pp. 121-128, Apr. 1986.

[8] R. E. Zulinski and J. W. Steadman, "Class E power amplifiers and frequency multipliers with finite dc-feed inductance," *IEEE Trans. on Circ. Syst.*, vol. CAS-34, pp. 1074-1084, Sept. 1987.

[9] R. Redl, B. Molnar, and N. O. Sokal, "Class E Resonant regulated dc/dc power converters: Analysis of operations, and experimental results at 1.5 MHz," *IEEE Trans. Power Elec.*, vol. PE-1, pp. 111-120, Apr. 1986.

[10] R. J. Gutmann, "Application of RF circuit design principles to distributed power converters," *IEEE Trans. Indust. Elec. Control Instr.*, vol. 27, pp. 156-164, Aug. 1980.

[11] M. K. Kazimierczuk and X. T. Bui, "Class E dc/dc converters with an inductive impedance inverter," *IEEE Trans. Power Elec.*, vol. 4, pp. 124-135, Jan. 1989.

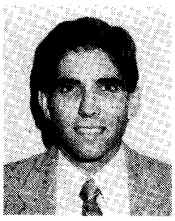

Philip R. Troyk (M'83-SM'91) received the B.S. degree in electrical engineering from the University of Illinois, Urbana, in 1974, and the M.S. and Ph.D. degrees in bioengineering from the University of Illinois, Chicago, in 1980 and 1983, respectively.

He was on the staff of Northrop Corporation, Rolling Meadows, IL, from 1973 to 1981. In 1983, he joined the faculty of the Illinois Institute of Technology, where he is currently an Associate Professor in the Pritzker Institute of Medical Engineering and the Department of Electrical and Computer Engineering. His interests include the design and packaging of electronic assemblies for implantation in the human body, and polymeric protection of thin film devices operating in high humidity environments.

Dr. Troyk is a member of Phi Kappa Phi, and the American Chemical Society.

Martin A. K. Schwan was born in Chicago, IL, in 1965. He received the B.S. and M.S. degrees in electrical engineering from the Illinois Institute of Technology, Chicago, in 1988 and 1991, respectively. At present he is pursuing the Ph.D. degree in electrical engineering at IIT.

In 1989 he joined the Pritzker Institute of Medical Engineering at IIT as a research assistant. His primary research at PIME is the design of transcutaneous coil drivers for providing power and data to implanted micro-neuromuscular stimulators. His other interests include: switch mode power converters and circuit design for implantable electronic devices.